sequences of benzylation, which blocks matrix-immobilizing hydrogen-bonding groups,[8] increasing backbone functionalization, which not unexpectedly enhances chain mobility,[9] and thermal epoxide cross-linking, which clearly has the greatest inhibitory effect on chain mobility. The second harmonic coefficients, measured at 25 °C within 10 min of cessation of poling, are relatively large, reflecting both the sizable chromophore number densities[2,4] as well as the anticipated $\mu\beta_{vec}$ value of HNPP.[6]

The temporal characteristics of d_{33} ($d_{33}(t)$) for the films prepared in this study are shown in Figures 1 and 2. The data in Figure 1 clearly indicate the diminution in SHG efficiency temporal stability incurred at very large chromophore functionalization levels. The data in Figure 2 compare $d_{33}(t)$ behavior for four HNPP-PHS-based systems, having (i) no protection or cross-linking, (ii) HNPP protection (BNPP) but no cross-linking, (iii) HNPP protection (BNPP) and cross-linking at the PHS backbone hydroxyl residues only, and (iv) cross-linking at both HNPP and PHS backbone positions. Several trends are evident. First, while T_g values afford a gross index of matrix mobility, they provide only a qualitative guide to the temporal stability of SHG efficiency (cf. i versus ii). The data show that any hydroxyl–hydroxyl hydrogen-bonding interactions involving the chromophore moieties have little if any effect on $d_{33}(t)$ over and above those provided by the polymer backbone hydroxyl moieties. Although cross-linking at the PHS functionalities alone (iii) affords a significantly lower T_g material than HNPP-PHS (i), the effect on $d_{33}(t)$ is clearly the opposite and large (Figure 2). Finally, cross-linking that *directly involves* the chromophore substituent affords the greatest stabilization of SHG efficiency (and correspondingly, the highest T_g).

The $d_{33}(t)$ data were fit by nonlinear regression methods[10] to a biexponential expression (eq 1)[2,4] that can be

$$d_{33} = Ae^{-t/\tau_1} + (1 - A)e^{-t/\tau_2} \qquad (1)$$

viewed as a "two-state" description of chromophore reorientation rates, e.g., in "liquidlike" and "glasslike" regions of the matrix.[11-14] Derived short-term and long-term decay time constants as well as A values are set out in Table I. These quantitatively amplify the above discussion, with the τ_2 values/SHG temporal stability parameters rivalling

those of any other known NLO chromophore-functionalized glassy polymer system.

These results provide the first information for a chromophore-functionalized glassy NLO polymer on the sensitivity of SHG temporal stability to the exact nature and position of hydrogen-bond/thermal cross-link points. It can be seen that these structural features can considerably modify, and can be employed to enhance, $d_{33}(t)$ characteristics, and in ways that are not necessarily obvious from T_g data alone.

Poled Polymeric Nonlinear Optical Materials. Enhanced Second Harmonic Generation Temporal Stability of Epoxy-Based Matrices Containing a Difunctional Chromophoric Co-Monomer

Michael A. Hubbard and Tobin J. Marks*

*Department of Chemistry and
the Materials Research Center
Northwestern University
Evanston, Illinois 60208-3113*

Weiping Lin and George K. Wong*

*Department of Physics and Astronomy and
the Materials Research Center
Northwestern University
Evanston, Illinois 60208-3113*

*Received March 17, 1992
Revised Manuscript Received June 23, 1992*

The long-term orientational stabilization of nonlinear optical (NLO) chromophores which have been preferentially aligned within a polymeric medium by electric field poling represents a crucial test of the extent to which polymer relaxation/physical aging can be controlled chemically and is of paramount importance to the development of efficient polymer-based second-order NLO materials.[1] We recently reported[2] an effective approach to chromophore immobilization which utilizes electric-field-induced alignment of high-β_{vec} chromophores dispersed within a two-component epoxy matrix[3] which is

(8) For discussions of the importance of hydrogen bonding in poly(p-hydroxystyrene) structure and chain dynamics, see: (a) Moskala, E. J.; Varnell, D. F.; Coleman, M. M. *Polymer* 1985, *26*, 228–234. (b) Nakamura, A.; Hatakeyama, T.; Hatakeyama, H. *Polymer* 1981, *22*, 473–476. (c) Hatakeyama, T.; Nakamura, A.; Hatakeyama, H. *Polymer* 1978, *19*, 593–594.

(9) (a) Rudin, A. *The Elements of Polymer Science and Engineering*; Academic Press: New York, 1982; Chapter 11. (b) Rabek, J. T. *Experimental Methods in Polymer Chemistry*; Wiley: New York, 1980; Chapter 32.

(10) Typical r values for the fits were in the range 0.98–0.99. Nevertheless, the accuracies of quantities representing extremely large τ_2 values are adversely affected by the necessarily limited duration of the data collection.

(11) Torkelson, J. M., private communication.

(12) Yu, W.-C.; Sung, C. S. P.; Robertson, R. E. *Macromolecules* 1988, *21*, 355–364 and references therein.

(13) (a) The $d_{33}(t)$ data could be fit at a similar level of confidence (r = 0.98–0.99) to the more phenomenological Kohlrausch–Williams–Watts stretched exponential expression:[13b-e]

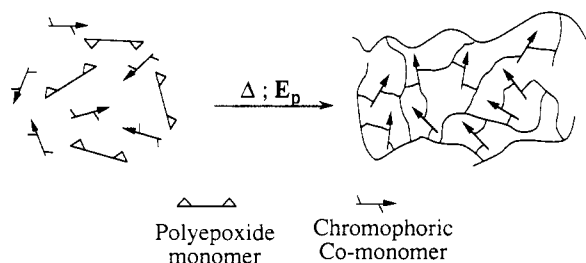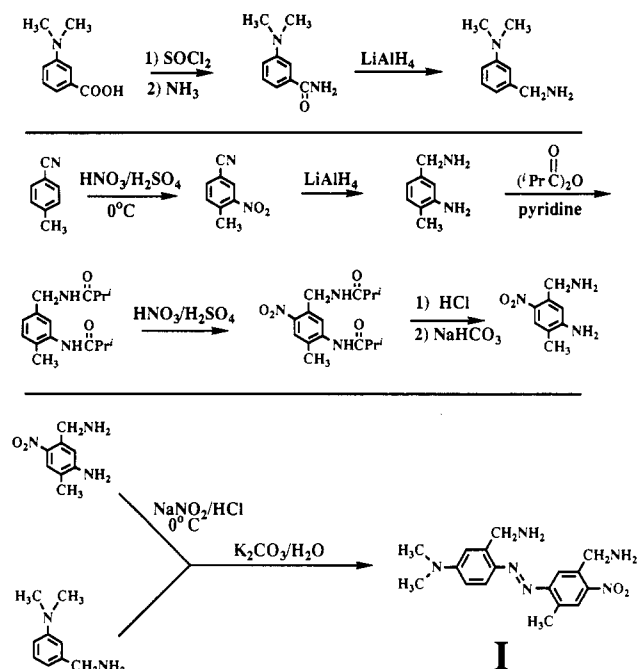$$d_{33} = e^{-(t/\tau)^\beta} \quad (0 < \beta \le 1) \qquad (2)$$

Derived β values for the cross-linked materials (0.78–0.85) at 25 °C suggest some degree of three-dimensional character.[14] (b) Frederickson, G. H.; Brawer, S. A. *J. Chem. Phys.* 1968, *84*, 3351–3366. (c) Shlesinger, M. F.; Montroll, E. W. *Proc. Natl. Acad. Sci. U.S.A.* 1984, *81*, 1280–1283. (d) Montroll, E. W.; Bendler, J. T. *J. Statist. Phys.* 1984, *34*, 129–162. (e) Williams, G.; Watts, D. C. *Trans. Faraday Soc.* 1970, *66*, 80–87.

(14) Fredrickson, G. H. *Annu. Rev. Phys. Chem.* 1988, *39*, 149–180.

(1) (a) *Materials for Nonlinear Optics: Chemical Perspectives*; Marder, S. R., Sohn, J. E., Stucky, G. E., Eds.; ACS Symposium Series 455; American Chemical Society: Washington, DC, 1991. (b) *Nonlinear Optical Properties of Organic Materials IV*; Singer, K. D., Ed.; *SPIE Proc.* 1991, *1560*. (c) Prasad, P. N.; Williams, D. J. *Introduction to Nonlinear Optical Effects in Molecules and Polymers*; Wiley: New York, 1991. (d) *Nonlinear Optical Properties of Organic Materials III*; Khanarian, G., Ed.; *SPIE Proc.* 1991, *1337*. (e) *Nonlinear Optical Properties of Organic Materials II*; Khanarian, G., Ed.; *SPIE Proc.* 1991, *1147*. (f) *Nonlinear Optical Effects in Organic Polymers*; Messier, J., Kajar, F., Prasad, P. N., Ulrich, D., Eds.; Kluwer Academic Publishers: Dordrecht, 1989. (g) *Organic Materials for Nonlinear Optics*; Hann, R. A., Bloor, D., Eds.; Royal Society of Chemistry: London, 1988.

(2) (a) Dai, D.-R.; Hubbard, M. A.; Li, D.; Park, J.; Ratner, J. A.; Marks, T. J.; Yang, J.; Wong, G. K. In ref 1a, pp 226–249 and references therein. (b) Hubbard, M. A.; Marks, T. J.; Yang, J.; Wong, G. K. *Chem. Mater.* 1989, *1*, 167–169. (c) Hubbard, M. A.; Minami, N.; Ye, C.; Marks, T. J.; Yang, J.; Wong, G. K. *SPIE Proc.* 1988, *971*, 136–143.

966 *Chem. Mater., Vol. 4, No. 5, 1992*

Communications

Scheme I. Reactive Chromophoric Comonomer Approach to NLO Epoxy Matrices

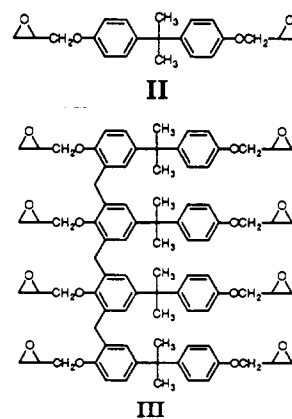**Scheme II. Synthesis of Azo NLO Comonomer I**

Table I. Second Harmonic Generation Frequency Doubling Efficiency and Temporal Stability Parameters for Corona-Poled Cross-Linked Matrices of Chromophore I and Epoxide Reagents II and III

material	T_g (°C)[a]	d_{33}[d] (10^{-9} esu)	τ_1 (days)[b]	τ_2 (days)[c]	A^c
I + II (25 °C)	121[d]	6.5	6.0	120	0.34
I + III (25 °C)	e	14.3	4.1	>300	0.29
I + III (85 °C)	e	20.3	1.6	120	0.47

[a] For materials cross-linked as described in the text. Measured at a heating rate of 10 °C/min. [b] At $\hbar\omega$ = 1.17 eV. [c] See eq 1 in text. [d] Very weak transition observed. [e] No transition observed.

The high-β_{vec} azo chromophore I was synthesized according to the reaction sequence outlined in Scheme II. All intermediates as well as I were characterized by standard spectroscopic and analytical techniques.[6] Three molecular design issues were addressed in the invention of this chromophore as the reactive co-monomer. Substituted azo compounds with electron-donating and -accepting substituents in the 4,4′ positions were selected since such structures are known to exhibit large π-electron-based β_{vec} values.[1,7] Second, two reactive amine functionalities were placed along the chromophore dipole moment direction to maximize incorporation of the chromophore into the matrix and to impede $\chi^{(2)}$-eroding reorientation processes transverse to the dipole moment direction. Third, aminomethyl rather than amino moieties were chosen so that the reactive functional groups would be electronically decoupled from the chromophore π electron system.

The effects of both monomeric (II)[8] and oligomeric (III)[9] diepoxide reagents (derivatives of diglycidyl ether of bisphenol A) were investigated in the poling/matrix formation process. Reaction mixtures of the difunctional chromophoric co-monomer I and the appropriate di-polyepoxide

concurrently subjected to thermal cross-linking.[4] The chromophores are found to exhibit higher levels of orientational stability within the cross-linked matrix, as evidenced by significantly improved second harmonic generation (SHG) temporal stability. Nevertheless, the SHG efficiency of such guest–host systems is severely limited by the low chromophore number densities and still less than optimum chromophore immobilizations which are practicable.[2,5] We communicate here the synthesis and implementation of a second generation epoxy-based NLO chromophore system in which a reactive high-β_{vec} chromophore serves as *both* the NLO-active component and as the diamine cross-linking agent of the matrix (Scheme I). We also demonstrate that the SHG temporal stability of such materials can be enhanced significantly by employing an oligomeric epoxide reagent.

(3) (a) Lohse, F. *Makromol. Chem., Macromol. Symp.* **1987**, *7*, 1–16. (b) Oleinik, E. F. *Adv. Polym. Sci.* **1986**, *80*, 49–99. (c) Dušek, K. *Adv. Polym. Sci.* **1986**, *78*, 1–59. (d) Rozenberg, B. A. *Adv. Polym. Sci.* **1986**, *75*, 113–165.

(4) For subsequent cross-linking studies employing alternative starting materials, see: (a) Eich, M.; Reck, B.; Yoon, D. Y.; Willson, C. G.; Bjorklund, G. C. *J. Appl. Phys.*, **1989**, *66*, 3241–3247. (b) Park, J.; Marks, T. J.; Yang, J.; Wong, G. K. *Chem. Mater.* **1990**, *2*, 229–231. (c) Jungbauer, D.; Reck, B.; Twieg, R.; Yoon, D. Y.; Willson, C. G.; Swalen, J. D. *Appl. Phys. Lett.* **1990**, *56*, 2610–2612. (d) Chen, M.; Yu, L.; Dalton, L.; Shi, Y.; Steier, W. H. *Macromolecules* **1991**, *24*, 5421–5428. (e) Jin, Y.; Carr, S. H.; Marks, T. J.; Lin, W.; Wong, G. K. *Chem. Mater.*, previous paper in this issue.

(5) (a) Hampsch, H. L.; Yang, J.; Wong, G. K.; Torkelson, J. M. *Macromolecules* **1990**, *23*, 3640–3647 and references therein. (b) Hampsch, H. L.; Yang, J.; Wong, G. K.; Torkelson, J. M. *Macromolecules* **1990**, *23*, 3648–3654 and references therein. (c) Singer, K. D.; Sohn, J. E.; Lalama, S. J. *Appl. Phys. Lett.* **1986**, *49*, 248–250.

(6) ¹H NMR (CDCl₃) δ 1.80 (s, 4 H), 2.71 (s, 3 H), 3.14 (s, 6 H), 4.11 (s, 2 H), 4.30 (s, 2 H), 6.64 (d of d, 1 H, *J* = 2.8, 9.2 Hz), 6.69 (d, 1 H, *J* = 2.4 Hz), 7.65 (s, 1 H, *J* = 9.2 Hz), 7.84 (d, 1 H, *J* = 9.2 Hz), 8.00 (s, 1 H); ¹³C NMR (DMSO-d₆) δ 16.64, 39.81, 42.04, 42.78, 110.3, 110.4, 116.8, 117.6, 127.1, 134.6, 138.0, 140.6, 146.7, 146.9, 153.2, 153.4; UV–VIS (THF) λmax = 465 nm, εmax = 17 100 L mol⁻¹ cm⁻¹. Anal. Calcd for C₁₇H₂₂N₆O₂: C, 59.63; H, 6.47, N, 24.54. Found: C, 59.80; H, 6.25, N, 23.80.

(7) (a) Calculated via the ZINDO/SOS formalism:[7b–d] μ = 9.7 D; βvec ($\hbar\omega$ = 1.17 eV) = 114 × 10⁻³⁰ cm⁵ esu⁻¹. We thank Dr. D. A. Kanis for these calculations. (b) Kanis, D. R.; Ratner, M. A.; Marks, T. J. *Chem. Mater.* **1991**, *3*, 19. (c) Kanis, D. R.; Ratner, M. A.; Marks, T. J. *Int. J. Quantum. Chem.* **1992**, *43*, 61–82. (d) An experimental electric-field-induced second harmonic (EFISH) measurement on I in dioxane solution ($\hbar\omega$ = 1.17 eV) yields a μβvec value within 10% of that exhibited by the structurally similar, well-known azo chromophore disperse orange-1 (4-(4-phenylazo)-*N*-phenylaniline).

(8) Commercially available as EPO-TEK 301-2 from Epoxy Technology Inc., Billerica, MA.

(9) Commercially available as Epi-Rez SU8 (a mixture of oligomers containing principally the tetramer) from Rhone-Poulenc Inc., Specialty Resins Group, Louisville, KY. We thank Rhone-Poulenc for a sample of this reagent.

were prepared by dissolving both components in dry, distilled THF (1:1 stoichiometric ratio of N–H bonds to epoxide moieties). The solutions were then filtered repeatedly through a 5-μm syringe filter and cast onto the conductive surface of indium–tin oxide (ITO) coated glass. The solvent was allowed to evaporate slowly in a Class 100 laminar flow hood. The films (typically 1–2-μm thickness) were then partially cross-linked by heating in vacuo for 3 h at 100 °C to remove any residual solvent and to improve dielectric stability. Parallel T_g and FT-IR monitored experiments with films cast on KBr plates were employed to establish optimum cross-linking conditions.[10]

Corona poling of the films was next carried out at 130 °C for 2 h using a needle-to-film distance of 1.0 cm and an applied corona potential of +5.0 kV.[11] The films were then cooled to room temperature over 1 h before removing the poling field, and the initial measurement of SHG properties made within 15 min of field removal. SHG measurements on the films at 1.064 μm were taken at room temperature in the p-polarized geometry and were referenced against quartz using procedures and instrumentation described previously.[12] Unpoled samples exhibited no SHG signal. Samples for time-dependent measurements at room temperature were stored in a desiccator. Those used for decay measurements at elevated temperature were stored under air in a thermostated tube furnace. Films were removed from the furnace and allowed to cool to ambient temperature before SHG measurements.

In Table I are compiled glass transition temperature (T_g) data and initial ($t \leq 15$ min) SHG coefficients (d_{33}) for the poled chromophore–epoxy matrices examined in this study. The T_g data reflect both a high degree of matrix vitrification/immobilization[3] and documented effects of epoxide multifunctionality.[3] The d_{33} values are relatively high, exceeding those of analogous guest–host materials ($(0.1 - 1.0) \times 10^{-9}$ esu)[2,5] by an order of magnitude or more. Nevertheless, the present film nonlinearities are somewhat less than might be expected on the basis of the chromophore $\mu\beta_{vec}$ value[7] and estimated number density ($\sim 6 \times 10^{20}$ cm^{-3}). Film optical spectra and the effects of varying the poling atmosphere[13] suggest that this result is unlikely to be a consequence of chromophore chemical degradation. Rather, it may be that a nonnegligible fraction of the chromophores are partially immobilized under the prepole cross-linking procedure (necessary to support the corona charge), hence slowly responsive or unresponsive to the electric field. Alternatively, the matrix densification process may be accompanied by a β_{vec}-diminishing[14] twist of the chromophore architecture from aryl ring coplanarity (not obvious from the optical spectra).
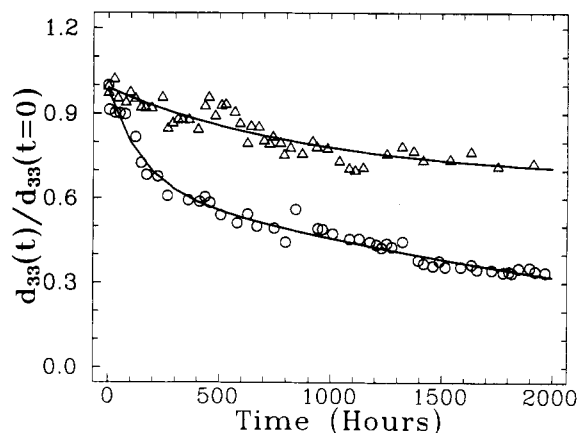

Figure 1. SHG temporal characteristics at 25 °C for two cross-linked films prepared from reactive NLO chromophore I and polyepoxide reagents III ($\triangle$) and II, ($\bigcirc$). The solid curves denote a nonlinear least-squares fit of the data to eq 1.
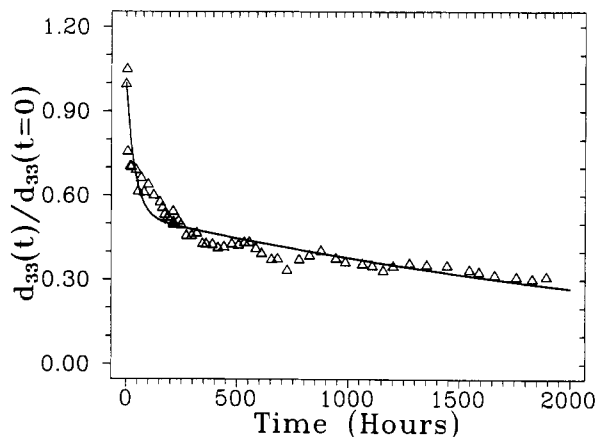

Figure 2. SHG temporal characteristics at 85 °C for a cross-linked film prepared from reactive NLO comonomer I and III. The solid curves denote a nonlinear least-squares fit of the data to eq 1.

The room-temperature SHG temporal stability characteristics of poled, cross-linked I + II and I + III films are shown in Figure 1. Qualitatively, it can be seen that the $d_{33}(t)$ stability characteristics of the chromophoric comonomer matrices equal or exceed those of previously described guest–host systems.[2,5] Furthermore, the superior immobilization characteristics of the polyepoxide-based matrices mirrors the disappearance of the T_g feature. The $d_{33}(t)$ data can be fit by nonlinear regression techniques to a phenomenological biexponential relationship (eq 1),

$$d_{33} = Ae^{-t/\tau_1} + (1 - A)e^{-t/\tau_2} \qquad (1)$$

which expresses the temporal characteristics in terms of a "two-state" matrix having, e.g., "liquidlike" and "glasslike" chromophore microenvironments.[15–18] Derived

(10) (a) McAdams, L. V.; Gannon, J. A. In *Encyclopedia of Polymer Science and Engineering*; Wiley: New York, 1986; Vol. 6, pp 322–382 and references therein. (b) Mertzel, E.; Koenig, J. L. *Adv. Polym. Sci.* **1986**, *75*, 74–112. (c) As judged from the intensity of the epoxy 916-cm^{-1} skeletal mode versus an internal standard, cross-linking is ~50% complete after 3 h at 100 °C. Complete cross-linking, as indicated by complete ($\geq$90%) disappearance of the 916-cm^{-1} feature, is observed after an additional 5 h at 100 °C or 1 h at 140 °C. DSC reveals no change in the observed T_g after cross-linking for 1 h at 140 °C.

(11) These conditions represent the most effective compromise between maximizing cross-linking temperature and poling field versus incurring significant dielectric breakdown and film damage.

(12) (a) Dai, D.; Marks, T. J.; Yang, J.; Lundquist, P. M.; Wong, G. K. *Macromolecules* **1990**, *23*, 1894–1896. (b) Ye, C.; Minami, N.; Marks, T. J.; Yang, J.; Wong, G. K. *Macromolecules* **1988**, *21*, 2901–2904. (c) Ye, C.; Marks, T. J.; Yang, J.; Wong, G. K. *Macromolecules* **1987**, *20*, 2322–2324.

(13) The NLO and temporal characteristics of the resulting films are insensitive to poling atmosphere (air or N$_2$).

(14) (a) Li, D.; Marks, T. J.; Ratner, M. A. *J. Phys. Chem.*, in press. (b) Li, D.; Marks, T. J.; Ratner, M. A. *Mater. Res. Soc. Symp. Proc.*, **1989**, *134*, 665–671.

(15) Torkelson, J. M., private communication.

(16) Yu, W.-C., Sung, C. S. P.; Robertson, R. E. *Macromolecules* **1988**, *21*, 355–364 and references therein.

(17) (a) The data could be fit at a similar level of confidence ($r = 0.96$) to the phenomenological Kohlrausch–Williams–Watts stretched exponential expression (eq 2).[17b-e] The derived β values (0.50–0.63 at 25 °C;

$$d_{33} = e^{-(t/\tau)^\beta} \quad (0 < \beta \leq 1) \qquad (2)$$

0.28 at 85 °C) which suggest three-dimensional character at 25 °C, also indicate that a single relaxation mechanism is not sufficient to describe the temporal characteristics. Furthermore, the decreased β observed with increased film storage temperature suggests that additional relaxation modes become relevant at elevated temperatures.[18] (b) Frederickson, G. H.; Brawer, S. A. *J. Chem. Phys.* **1986**, *84*, 3351–3366. (c) Shlesinger, M. F.; Montroll, E. W. *Proc. Natl. Acad. Sci. U.S.A.* **1984**, *81*, 1280–1283. (d) Montroll, E. W.; Bendler, J. T. *J. Statist. Phys.* **1984**, *34*, 129–162. (e) Williams, G.; Watts, D. C. *Trans. Faraday Soc.* **1970**, *66*, 80–87.

τ_1, τ_2, and A parameters ($r \geq 0.96$) are set out in Table I. The impressive SHG temporal stability of the I + III cross-linked matrices prompted additional quantitative temporal stability measurements at elevated temperatures. As can be seen in Figure 2 and Table I, the d_{33} decay (especially the initial decay) is, as expected, more rapid at 85 °C. Nevertheless, the long-term decay time constant is still on the order of 4 months.

These results demonstrate that difunctional chromophoric azo co-monomers which can function as amino components of cross-linkable NLO-active epoxy matrices are synthetically accessible. After concurrent electric field poling and thermal cross-linking with a diepoxide or preferentially, with a polyepoxide, such matrices exhibit high SHG efficiency and SHG efficiency temporal stability.

---

(18) Fredrickson, G. H. *Annu. Rev. Phys. Chem.* **1988**, *39*, 149–180.

Room-Temperature Synthesis of Molybdenum and Tungsten Carbides, Mo₂C and W₂C, via Chemical Reduction Methods

D. Zeng and M. J. Hampden-Smith*

Department of Chemistry and Center for Micro-Engineered Ceramics University of New Mexico Albuquerque, New Mexico 87131

The preparation of nanometer-sized particles of phase-pure materials is currently attracting intense interest in materials chemistry because such particles exhibit unique chemical and physical properties that are intermediate between those of molecules and extended solids.[1] For example, metal chalcogenides exhibit size-dependent physical properties in the 2–100-nm size regime[2] and metal particles exhibit size-dependent selectivity[3] and reactivity[3,4] in catalytic reactions. However, traditional solid-state synthetic methods seldom result in formation of particles smaller that 100 nm.[5] New synthetic routes based on chemical methods show promise for the formation of materials with a homogeneity, morphology, composition, microstructure, and purity not otherwise obtainable. For example, the reduction of metal salts in the presence of a surfactant, often in inverse micelles, has led to formation
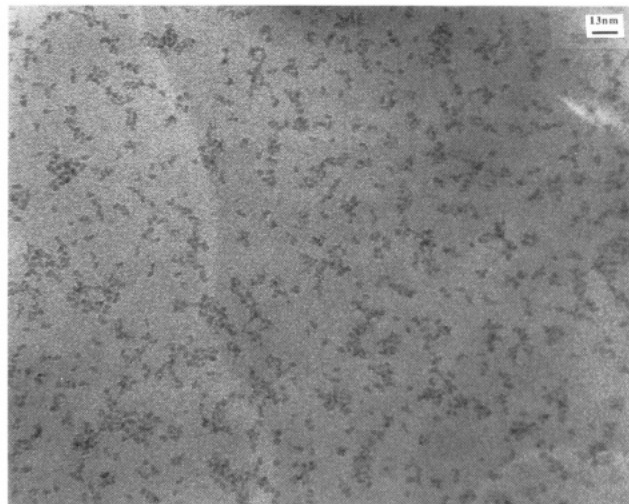

Figure 1. TEM data for Mo₂C particles formed by reduction of MoCl₃(THF)₃ with LiBEt₃H in THF.

of monodispersed nanometer-sized particles.[6] However, the surfactant can lead to impurity incorporation in subsequent steps and as a result a number of groups are investigating alternative synthetic strategies. Reicke et al.[7] have extensively investigated the reduction of metal salts with alkali-metal naphthalenides and formed highly dispersed, reactive metal powders. Bonnemann et al.[8,9] have shown that trialkylborohydride reducing agents can be used to reduce a variety of metal complexes to form the corresponding metal colloids. The metals are reasonably pure (70–98%), the particle size was approximately 10–100 nm and generally crystalline materials were formed depending on the specific system as determined by X-ray diffraction.

Here we report the room-temperature reduction of molybdenum and tungsten halides with LiBEt₃H, which results in the formation of monodispersed, 1- and 2-nm Mo₂C and W₂C colloids, respectively, rather than formation of the metal. Existing routes to these interstitial carbide materials involve either high temperature (>1200 °C) reduction of the corresponding metal oxide[10–13] or halide[14] or ball-mixing mixtures of elemental powders for extended periods at lower temperatures.[15,16] Both these methods often result in addition reactions between the reagent and container causing impurity incorporation.

The reduction of THF suspensions of MoCl₄(thf)₂, MoCl₃(thf)₃ and WCl₄ at −10 °C with a slight excess of the stoichiometric amount of LiBEt₃H resulted in the forma-

---

* To whom correspondence should be addressed.

(1) See, e.g. Frontiers in Materials Science. *Science* **1992**, *255*, 1049 and references therein.

(2) Pool, R. *Science* **1990**, *248*, 1186 and references therein.

(3) Che, M.; Bennett, C. O. *The Influence of Particle Size on the Catalytic Properties of Supported Metals. Adv. Catal.* **1989**, *36*, 55. See also: Glassl, H.; Hayek, R.; Kramer, R. *J. Catal.* **1981**, *68*, 397.

(4) Davis, S. C.; Klabunde, K. J. *Chem. Rev.* **1982**, *83*, 153.

(5) Chorley, R. W.; Lednor, P. W. *Adv. Mater.* **1991**, *3*, 474.

(6) Wilkoxon, T. P.; Baughmann, R. J.; Williamson, R. L. *Synthesis and Properties of New Catalysts: Utilization of Novel Materials Components and Synthetic Techniques.* Corcoran, E. W., Ledoux, M. J., Eds.; Fall Materials Research Society Meeting, Boston, MA, 1990 and references therein.

(7) Riecke, R. D. *Science* **1989**, *246*, 1260. Riecke, R. D.; Burns, T. P.; Wehmeyer, R. M.; Kahn, B. E. In *High Energy Processes in Organometallic Chemistry*; ACS Symposium Series 333; American Chemical Society: Washington, DC, 1987.

(8) Bonneman, H.; Brijoux, W.; Jousson, T. *Angew. Chem., Int. Ed. Engl.* **1990**, *29*, 273.

(9) Bonneman, H.; Brijoux, W.; Brinkmann, R.; Dinjus, E.; Jousson, T.; Korall, B. *Angew. Chem., Int. Ed. Engl.* **1991**, *30*, 1312.

(10) Lee, J. S.; Oyama, S. T.; Boudart, M. *J. Catal.* **1987**, *106*, 125.

(11) Oyama, S. T.; Schlatter, J. C.; Metcalfe III, J. E.; Lambert, J. M. *Ind. Chem. Res.* **1988**, *27*, 1639.

(12) Boudart, M.; Oyama, S. T.; Volpe, L. US Patent 4,515,763.

(13) Ranhorta, G. S.; Haddix, G. W.; Bell, A. T.; Reimer, J. A. *J. Catal.* **1987**, *108*, 24.

(14) Tamari, N.; Kato, A. *Yogyo Kyokaishi* **1976**, *409*, 84; *Chem. Abstr.* 85:162594d.

(15) Le Caer, G.; Bauer-Grosse, E.; Pianelli, A.; Bouzy, E.; Matteazzi, P. *J. Mater. Sci.* **1990**, *23*, 4726.

(16) Matteazzi, P.; Le Caer, G. *J. Am. Ceram. Soc.* **1991**, *74*, 1382.